Liquid crystal gratings based on alternate TN and PA photoalignment

Wei Hu,[1,2] Abhishek Srivastava,[2] Fei Xu,[1] Jia-Tong Sun,[2] Xiao-Wen Lin,[1] Hong-Qing Cui,[3] Vladimir Chigrinov[2,4] and Yan-Qing Lu[1,*]

[1]*College of Engineering and Applied Sciences and National Laboratory of Solid State Microstructures, Nanjing University, Nanjing 210093, China*
[2]*Center for Display Research, Department of Electronic and Computer Engineering, Hong Kong University of Science and Technology, Clear Water Bay, Kowloon, Hong Kong China*
[3]*LCD R&D Center, Infovision Optoelectronics Crop., Kunshan 215300, China*
[4] *eechigr@ust.hk*
[*] *yqlu@nju.edu.cn*

Abstract: A diffraction grating is proposed by periodically defining the liquid-crystal director distribution to form alternate parallel aligned and twist nematic regions in a cell placed between two crossed polarizers. Based on the combined phase and amplitude modulation, both 1D and 2D tunable gratings are demonstrated. Low voltage ON/OFF switching of 1st order diffracted light with extinction ratio over 80 is achieved within a small voltage interval of 0.15 V_{rms}. Unique four-state feature of the cell is obtained and their applications in optical logic devices are discussed.

©2012 Optical Society of America

OCIS codes: (160.3710) Liquid crystals; (050.1950) Diffraction gratings.

References and links

1. W. M. Gibbons and S. T. Sun, "Optically generated liquid crystal gratings," Appl. Phys. Lett. **65**(20), 2542–2544 (1994).
2. X. Zhao, A. Bermak, F. Boussaid, T. Du, and V. G. Chigrinov, "High-resolution photoaligned liquid-crystal micropolarizer array for polarization imaging in visible spectrum," Opt. Lett. **34**(23), 3619–3621 (2009).
3. E. Jang, H. R. Kim, Y. J. Na, and S. D. Lee, "Multistage optical memory of a liquid crystal diffraction grating in a single beam rewriting scheme," Appl. Phys. Lett. **91**(7), 071109 (2007).
4. X. W. Lin, J. B. Wu, W. Hu, Z. G. Zheng, Z. J. Wu, G. Zhu, F. Xu, B. B. Jin, and Y. Q. Lu, "Self-polarizing terahertz liquid crystal phase shifter," AIP Advances **1**(3), 032133 (2011).
5. Y. H. Wu, Y. H. Lin, Y. Q. Lu, H. W. Ren, Y. H. Fan, J. R. Wu, and S. T. Wu, "Submillisecond response variable optical attenuator based on sheared polymer network liquid crystal," Opt. Express **12**(25), 6382–6389 (2004).
6. J. Chen, P. J. Bos, H. Vithana, and D. L. Johnson, "An electro-optically controlled liquid crystal diffraction grating," Appl. Phys. Lett. **67**(18), 2588–2590 (1995).
7. W. Y. Wu and A. Y. G. Fuh, "Rewritable liquid crystal gratings fabricated using photoalignment effect in dye-doped poly(vinyl alcohol) film," Jpn. J. Appl. Phys., Part 1 **46**(10A), 6761–6766 (2007).
8. S. Y. Huang, S. T. Wu, and A. Y. G. Fuh, "Optically switchable twist nematic grating based on a dye-doped liquid crystal film," Appl. Phys. Lett. **88**(4), 041104 (2006).
9. Y. Q. Lu, F. Du, and S. T. Wu, "Polarization switch using thick holographic polymer-dispersed liquid crystal grating," J. Appl. Phys. **95**(3), 810–815 (2004).
10. D. Subacius, S. V. Shiyanovskii, P. Bos, and O. D. Lavrentovich, "Cholesteric gratings with field-controlled period," Appl. Phys. Lett. **71**(23), 3323–3325 (1997).
11. H. Q. Xianyu, S. Faris, and G. P. Crawford, "In-plane switching of cholesteric liquid crystals for visible and near-infrared applications," Appl. Opt. **43**(26), 5006–5015 (2004).
12. B. I. Senyuk, I. I. Smalyukh, and O. D. Lavrentovich, "Switchable two-dimensional gratings based on field-induced layer undulations in cholesteric liquid crystals," Opt. Lett. **30**(4), 349–351 (2005).
13. A. K. Srivastava, E. P. Pozhidaev, V. G. Chigrinov, and R. Manohar, "Single walled carbon nano-tube, ferroelectric liquid crystal composites: Excellent diffractive tool," Appl. Phys. Lett. **99**(20), 201106 (2011).
14. M. Bouvier and T. Scharf, "Analysis of nematic-liquid-crystal binary gratings with high spatial frequency," Opt. Eng. **39**(8), 2129–2137 (2000).
15. L. L. Gu, X. N. Chen, W. Jiang, B. Howley, and R. T. Chen, "Fringing-field minimization in liquid-crystal-based high-resolution switchable gratings," Appl. Phys. Lett. **87**(20), 201106 (2005).
16. R. G. Lindquist, J. H. Kulick, G. P. Nordin, J. M. Jarem, S. T. Kowel, M. Friends, and T. M. Leslie, "High-resolution liquid-crystal phase grating formed by fringing fields from interdigitated electrodes," Opt. Lett. **19**(9), 670–672 (1994).

17. J. Yan, Y. Li, and S. T. Wu, "High-efficiency and fast-response tunable phase grating using a blue phase liquid crystal," Opt. Lett. **36**(8), 1404–1406 (2011).
18. B. Wen, R. G. Petschek, and C. Rosenblatt, "Nematic liquid-crystal polarization gratings by modification of surface alignment," Appl. Opt. **41**(7), 1246–1250 (2002).
19. J. Kim, J. H. Na, and S. D. Lee, "Fully continuous liquid crystal diffraction grating with alternating semi-circular alignment by imprinting," Opt. Express **20**(3), 3034–3042 (2012).
20. V. Kapoustine, A. Kazakevitch, V. So, and R. Tam, "Simple method of formation of switchable liquid crystal gratings by introducing periodic photoalignment pattern into liquid crystal cell," Opt. Commun. **266**(1), 1–5 (2006).
21. H. Akiyama, T. Kawara, H. Takada, H. Takatsu, V. Chigrinov, E. Prudnikova, V. Kozenkov, and H. Kwok, "Synthesis and properties of azo dye aligning layers for liquid crystal cells," Liq. Cryst. **29**(10), 1321–1327 (2002).
22. V. Presnyakov, K. Asatryan, T. Galstian, and V. Chigrinov, "Optical polarization grating induced liquid crystal micro-structure using azo-dye command layer," Opt. Express **14**(22), 10558–10564 (2006).
23. I. C. Khoo and S. T. Wu, *Optics and Nonlinear Optics of Liquid Crystals* (World Scientific, Singapore, 1993).
24. N. Konforti, E. Marom, and S. T. Wu, "Phase-only modulation with twisted nematic liquid-crystal spatial light modulators," Opt. Lett. **13**(3), 251–253 (1988).
25. V. Chigrinov, A. Muravski, H. S. Kwok, H. Takada, H. Akiyama, and H. Takatsu, "Anchoring properties of photoaligned azo-dye materials," Phys. Rev. E Stat. Nonlin. Soft Matter Phys. **68**(6), 061702 (2003).
26. V. G. Chigrinov, V. M. Kozenkov, H. S. Kwok, *Photoalignment of Liquid Crystalline Materials: Physics and Applications* (Wiley, England, August 2008).
27. Y. A. Zaghloul and A. R. M. Zaghloul, "Complete all-optical processing polarization-based binary logic gates and optical processors," Opt. Express **14**(21), 9879–9895 (2006).
28. Y. X. Zhang, Y. P. Chen, and X. F. Chen, "Polarization-based all-optical logic controlled-NOT, XOR, and XNOR gates employing electro-optic effect in periodically poled lithium niobate," Appl. Phys. Lett. **99**(16), 161117 (2011).
29. J. H. Kim, M. Yoneya, and H. Yokoyama, "Tristable nematic liquid-crystal device using micropatterned surface alignment," Nature **420**(6912), 159–162 (2002).
30. Y. Q. Lu, X. Liang, Y. H. Wu, F. Du, and S. T. Wu, "Dual-frequency addressed hybrid-aligned nematic liquid crystal," Appl. Phys. Lett. **85**(16), 3354–3356 (2004).

1. Introduction

Due to the electrical switchability and tunability, passive elements and devices based on liquid crystals (LCs) have attracted intensive attentions [1–5]. Diffraction grating is one kind that has been well documented with either periodic amplitude or phase modulation. Among them, phase grating has the advantages of higher diffraction efficiency and better tunability [6–9], therefore most researches are focused on this type. Several fabrication strategies are commonly used for LC phase gratings. First is utilizing the natural ability of materials such as cholesteric LCs to form a field-controlled periodic bulk structure [10–13]. Second is employing arrays of parallel electrodes to generate longitudinal [14, 15] or lateral [15–17] periodic electric field distribution and locally control the directors of uniformly pre-aligned LCs. The third one is directly guiding the LC directors by alignment layers patterned through either mechanical methods [6, 18, 19] or photoalignment techniques [7, 8, 20], and further tuning with uniform external fields. Among all above techniques, photoalignment has been proved to be a promising approach with several advantages. Firstly, it facilitates arbitrary grating pattern designs and endows the gratings with hysteresis-free and fast response diffraction within whole VIS-IR spectrum range. Secondly, it simplifies the electrical driving and avoids the undesired diffraction effects resulting from initial periodical probes and fringe fields. Thirdly, it enables the creation of high quality LC alignment with resolution up to 1 μm [2, 20], without any mechanical damage, electrostatic charge or dust contamination [21].

Several gratings were proposed and demonstrated according to this technique. Based on the light-induced reorientation of azobenzene chromophores, an optically switchable twist-nematic grating was fabricated using a dye-doped LC cell [8]. Presnyakov *et. al.* realized a grating using azo-dye alignment layer exposed with two interfering laser beams of opposite circular polarizations [22]. Exploiting UV photoalignment and amplitude mask, Kapoustine *et al* demonstrated switchable LC gratings through introducing a periodical variation of the alignment directions into one substrate of cells [20]. Gratings based on 90° twist nematic (TN)/ parallel aligned (PA) periodical alignment and ± 45° TN reversely twisted periodical alignment were also presented through photoalignment patterning on one substrate [7].

Due to the electro-optic (EO) tunability of LC, the efficiencies of different diffraction orders thus are adjustable. The extreme case is that a specific order, *e.g.*, 1st order, is totally turned on and off at different driving voltages. To accomplish such a switching, phase change of at least one π must be achieved. Normally several volts voltage interval are required to fulfill an enough phase difference between on and off states. Attempts towards decreasing both the switching voltage and voltage interval are meaningful, which would reduce the power consumption and simplify the driven component.

In this work, a design of tunable LC gratings with alternating 90° TN regions and PA (45° with respect to the alignment direction of TN) is proposed, based on the combination of phase and amplitude modulation. Both 1D and 2D diffraction gratings are demonstrated by periodic photoalignment of sulfonic azo-dye (SD1) films with a linearly polarized light beam. The different voltage-dependent transmittances between adjacent regions make the device exhibiting four characteristic states. The combined modulation mode allows a very low manipulating voltage. Besides, the grating also has some advantages like simple and accurate fabrication, fast switching, high efficiency and high contrast ratio. In addition, the unique four-state feature may bring some new technical applications.

2. Design and fabrication

Alignment is necessary for all applications of nematic LCs. Both TN and PA are normally used aligning modes, exhibiting different EO properties including voltage-dependent phase changes and transmittances. In our design, micro TN and PA regions are assembled alternately to form gratings. The two regions present different phase changes along with external fields [23, 24]. When the cell is placed between two crossed polarizers, different output phases at adjacent PA and TN regions result in a grating profile. Besides, the transmittances of the adjacent regions also change differently with applied voltages [23], which induces an amplitude difference between the two regions. Thereby, for the proposed diffraction gratings, both phase and amplitude modulations are coupled and could be tuned by external fields.

Figure 1 shows the voltage dependent transmission (VT) curves of 6.0-μm-thick TN and PA LC cells respectively, filled with positive LC RDP-41063 (Dai-Nippon Ink and Chemicals). For the proposed cells, the transmittances and output phases of two adjacent regions could be tuned separately by the same uniform external fields. The insets conceptually reveal a unique four-state feature of such a cell: 'I' shows binary patterns when the transmittance of TN regions is 100% and that of PA ones is zero. As no light transmits through the PA regions, the cell at this state plays as a pure amplitude grating. 'II' is a bright state when both regions reach to the maximal transmittances. The cell here is a pure phase grating. 'III' is a pattern with reverse transmittances compared with 'I'. Similarly, the cell is a pure amplitude grating. Finally, 'IV' is a homogenously dark state (herein, 15 V or more, all given voltages are root mean square values), which is also an off state of the grating. Although only four states are listed, it's unambiguous that such an element could be continuously tuned by electric fields. By the way, all other states are the combination of phase and amplitude gratings. That suggests a novel design for switchable and tunable LC gratings.
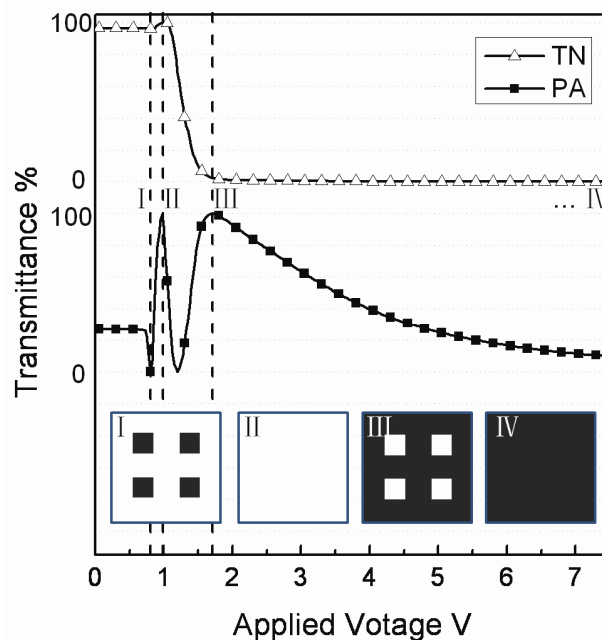
Fig. 1. VT curves of 6.0-μm-thick TN and PA LC cells between crossed polarizers separately. The front polarizer is at 0° and 45° to the LC director of TN cell and PA cell respectively. The insets conceptually reveal four states of this cell under different voltages.

Multi-domain alignment plays a significant role in achieving the desired LC director distribution. In present work, the photoalignment technique has been employed to accomplish the concept, and SD1 (Dai-Nippon Ink and Chemicals, Japan) is utilized as the alignment layer. The incident light is generated by a monochromatic blue LED (405 ± 10 nm, 40 mW/cm^2, Φ = 50 mm, precisely collimated by a lens) and linearly polarized by a nano-wire-grids polarizer, then normally irradiates onto SD1 films. SD1 molecules tend to align their absorption oscillators perpendicular to the polarization of the activating light [25] and then supply considerably high anchoring energy comparable to that of rubbed PI [21]. SD1 shows excellent alignment rewritability that the alignment of a pre-aligned cell can be altered by another irradiation with the same alignment quality [26]. This character makes the multi-domain alignment approach more practical.
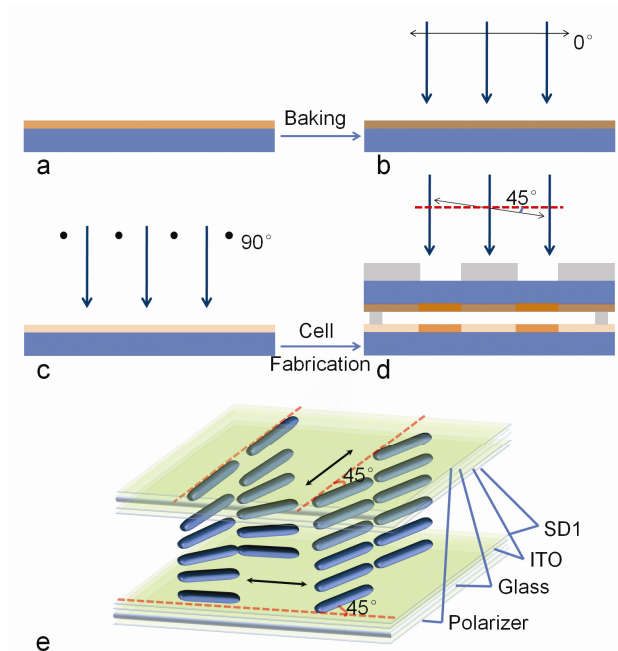
Fig. 2. Schematic drawing of photoalignment procedure: a) spincoating SD1, b-c) orthogonal photoalignment on two cell substrates, d) cell assembling and photopatterning with an amplitude mask, and e) cell structure and LC orientations in alternate TN-PA domains

The cell preparation is schematically illustrated in Fig. 2. SD1 was dissolved in N, N-dimethylformamide (DMF) at a concentration of 0.5 wt%. The solution was spin-coated on ITO-coated glass substrates (Fig. 2(a)). The two substrates were set orthogonal under linearly polarized light for an exposure dose of ca. 5 J/cm^2 (Fig. 2 (b) and 2(c)). Then the two substrates were assembled to form a 90°-TN cell with an average thickness of 6.0 μm. Afterwards, the cell was exposed again through an amplitude mask at 45° with respect to previous alignment direction. The exposed regions were realigned to PA, while the mask shadow domains still keep TN alignment (Fig. 2(d)). Thus the cell with alternate PA and TN domains has been constructed. Thereafter, LC was injected into the cell at isotropic phase. After cooling to room temperature, LC alignment in the cell is illustrated in Fig. 2(e). No precise adjustment is required here for all patterns were fabricated simultaneously in a single process, making the fabrication simple and accurate.

In our experiments, AC drivers supply 1 kHz rectangular signals with a duty cycle of 50% to samples. The VT curves were studied in the light path: a highly linearly polarized He–Ne laser (632 nm), which makes the system free of polarizer, the sample, an analyzer and a photodetector. The light beam is normally incident to the cell with its polarization direction parallel to front LC director in TN domains.

3. Experimental results

A replica structure of the mask with periodically alternate stripes (40 μm, to be TN) and spaces (10 μm, to be PA) were recorded in the LC cell. In Fig. 3(a), total transmittance of the cell versus voltage reveals the contributions from both TN and PA regions respectively at different applied votages, which is the overlap of V-T vures of the two regions separately. The contrast ratio (voltage dependent intensity of + 1st order divided by that of 0th) indicates the variations of diffraction efficiency along with external fields. Insets (taken under BH3-F04T Olympus microscope) demonstrate the expected four states: stripe pattern (PA domains are dark), bright state, reverse pattern (TN domains are dark) and state approaching uniform dark respectively. Transmission difference could still be observed in bright state due to the

limitation of applying voltage step. Patterns could be observed at 5 V; however, further increasing the voltage to 15 V would induce a homogeneously dark state. The curve in Fig. 3(b) exhibits a continuous intensity change of 1st order. Two peaks are observed in the curve, one is sharp and strong while the other is wide and weak. The diffraction efficiency of 1st order reaches 12.0% as compared to the total intensity of transmitted light at voltage-off-state. Insets (Media 1) are the diffraction patterns at different voltages, which explicitly illustrate the tunability of the gratings.
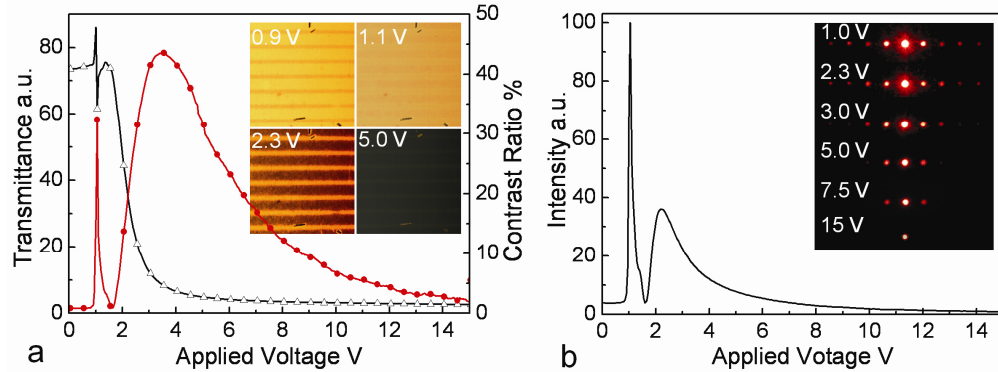

Fig. 3. a) VT curve of the cell (hollow triangles and line) and contrast ratio between voltage dependent intensity of 1st and 0th orders (solid circles and line). Insets show the four states respectively (all image sizes are $350 \times 350 \ \mu m^2$), b) intensity of 1st order as a function of driving voltage. Insets (Media 1) show the diffraction patterns at different voltages.

The extinction ratio (ER, intensity maximum over minimum) of 1st order reaches over 120 in the whole voltage range (0-15 V). Furthermore, ER over 30 is achieved within the voltage interval of 0.15 V at very low operating voltage (0.80 V to 0.95 V), which permits a rapid switching. The switching on and off time herein are defined as 10% to 90% in transmittance and reverse. The measured values of 1st order in the low voltage range are 6.5 ms and 36 ms separately.
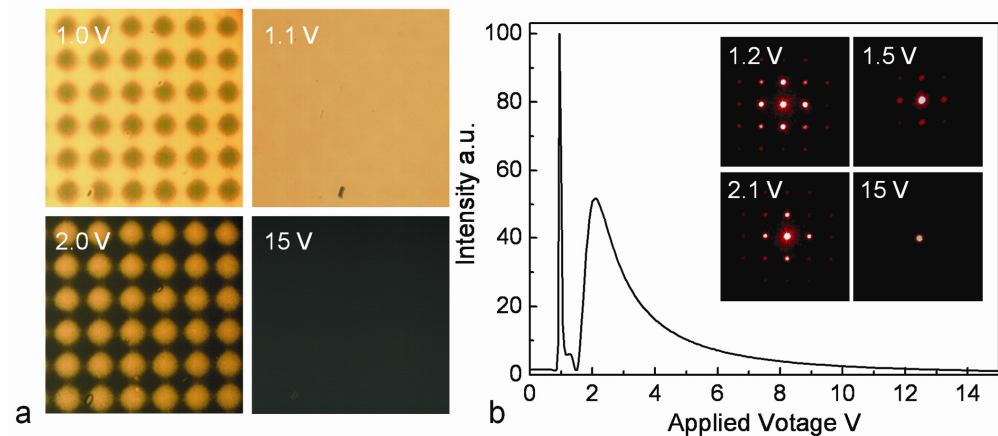

Fig. 4. a) four states of 2D TN-PA cell (all image sizes are $300 \times 300 \ \mu m^2$), b) intensity of 1st order as a function of driving voltage, insets (Media 2) show the diffraction patterns at different voltages.

2D diffraction grating is presented as well, which is especially meaningful for beam multiplexing that distributes an optical signal into an array of receivers [12]. A photo mask with $25 \times 25 \ \mu m^2$ square-hole-arrays in metal grids was employed. However, due to beam size expansion and LC disclination, the pattern looks more like circular disks. As shown in Fig.

4(a), dark PA domains are separated by bright TN regions at 1.0 V. A homogeneously bright state was achieved exactly at 1.1 V. It is attributed to the cell gap variation (ca. 0.3 μm among cells) compared to above 1D grating. Dark grids and bright PA "squares" were observed at 2.0 V. At 15 V, LC molecules were all vertically aligned by external field and exhibited a uniform dark state. The curve in Fig. 4(b) shows voltage dependency of the intensity for the 1st order, which is similar to that of 1D grating. The diffraction efficiency of 1st order reaches 18.2%. ER over 140 of 1st order is achieved in the whole voltage range and it exceeds 80 with voltage applied from 0.80 V to 0.95 V. The four insets in Fig. 4(b) (Media 2) prove the switching and tuning of the grating. Small scattering has been observed during test. The scattering is due to the disclinations of LC molecules during rapid voltage changing, which can be explained as follows. With the absence of chiral dopant, turning left or right from initial direction would be identical for TN aligned LC, resulting coexistence of counter-helical domains. These domain boundaries would cause LC disordering as well as the TN-PA interfaces do. That makes a random leakage of light and results in scattering. However, it does not degrade the performance evidently according to our experimental results.

4. Discussions

Experimental results reveal a small voltage interval of 0.15 V for the switching. It is reduced over one order as compared with normal LC gratings. Moreover, the switching is accomplished under a low operating voltage below 1 V with a high ER up to 80. It indicates the device could be directly driven by a low voltage output DC (direct current) source without inducing any electrochemical instability to LCs. That means the presented gratings could be driven by single button battery or simple photovoltaic cells, which is significantly meaningful for the widely used portable optical switches and switch arrays. Besides the simplification of driven component, the novel design could also reduce the power consumption remarkably. This feature will be more beneficial for LC devices operating in infrared band for some long-wavelength photonic applications [4, 5].

We attribute the superiority to the unique mechanism of combined phase and amplitude modulation. In our design, the gratings are formed by two aligning modes (90° TN and PA). The two regions exhibit distinct phase changes along with external fields [23, 24]. Normally people focus more on the transmittance of TN cell at different voltages, while actually the phase of the light also experiences large scale fluctuation just above the threshold [24]. Compared with previous configurations, our design takes both the intensity and special phase change of TN alignment into account. The asynchronous variations of phase and amplitude between TN and PA regions are very unique when the grating is placed between crossed polarizers. It results in dramatically varied diffraction curves in Fig. 3(b) and Fig. 4(b) at around 1 volt. As a consequence, our grating is different from the pure phase type, the diffraction of which may only be switched on and off through enough phase change. It also avoids the intrinsic disadvantages of pure amplitude gratings such as low efficiency and poor tunability. The intensity of diffraction orders is determined by both phase and light intensity contrasts in different domains, which give rise to the steep modulation and high contrast of 1st order diffraction at low voltages.

The variation of diffraction order intensities could be manipulated by adjusting the EO properties of the two adjacent domains. To be more specific, device performance can be further improved by tuning the filling factor of photo masks, cell gap, LC birefringence, relevant elastic constants and other material and cell parameters. In present work, both the diffraction efficiency and low voltage ER of 2D grating are significantly improved in comparison with 1D grating. The improvement is due to the cell gap and filling factor variations. It confirms above assumption that further performance optimizing of such gratings is achievable.

Besides the combined modulation and unique performance, the proposed gratings have another characteristic with respect to the common ones, which are usually patterning aligned only one substrate of the cell and leave the other uniformly aligned [6, 14, 18–20, 22]. Herein both inner sides of the cell are photopatterned simultaneously. The design provides a

rectangular-like phase profile that would distribute light into higher diffraction orders. In our experiments, the scattering is well controlled and its influence to the device performance is negligible. We consider the reasons are the well formed rectangular profile and good alignment quality, which restrict the size of boundaries. Although only simple 1D and 2D diffraction gratings are demonstrated in this work, since the initial spatial distribution of LC directors is determined only by photo patterning, arbitrary patterns could be accomplished easily. The proposed design with potential of high-resolution could be applied to a wide field of tunable optical elements and devices, such as optical interconnects, beam steering devices and spatial light modulators.

Due to the combination of phase and amplitude modulation, our photo-aligned LC TN/PA grating shows some advantages over normal tunable gratings. However, the unique four-state feature due to asynchronous TN/PA voltage responses may still have some other interesting applications, for example, in the amplitude or polarization based logic gates and optical processors [27,28]. From Fig. 1, we may define the logic 0 (L0) to be dark state or horizontal polarization state. The logic 1 (L1) is set to be bright state or vertical polarization state. Therefore in a period or a unit with both TN and PA regions, the four states at voltages, V_I-V_{IV}, just correspond to the combined logic states (1, 0), (1, 1), (0, 1) and (0, 0), respectively. And, if an identical LC cell is placed behind it, different logic states and gates thus could be implemented by just tuning the voltage on a certain unit. For example, for the input state of (1, 0) with vertical polarization and horizontal polarization in TN and PA regions, applying V_I-V_{IV} give rise to (0, 0), (0, 1), (1, 1) and (1, 0) states, respectively. These results are quite similar to the proposals to generate all types of binary gates, including AND, NAND, OR, NOR, XOR, XNOR, in [27], but with much simpler optical architectures. The two beams route [27] is replaced by a single TN/PA unit with uniform driving voltage. Complicated beam splitters and discrete polarization controlling elements are saved. Moreover, for a LC grating with multi periods or units, multiple-input-multiple-output logic processors thus are also achievable. If more complicated alignment states are induced into a unit rather than just TN and PA [19, 29], ternary optical devices [29, 30] are even expected.

5. Conclusion

A switchable LC grating based on combined phase and amplitude modulation of alternate TN/PA regions is proposed. It consists of two planar continuous electrodes, a sandwiched nematic LC layer, and crossed polarizers. Both 1D and 2D gratings were produced through photoalignment with an amplitude mask. The intensities of diffraction orders could be controlled by uniform external field. For the proposed gratings, advantages such as, easy manufacturing, low switching voltage and unique four-state feature were realized. Fast and large switchability was achieved at very low operating voltage. It supplies a new approach for low power consumption and driven source simplified LC photonic devices. In addition, based on the four-state feature, the presented cell exhibits broadly potential applications in optical logic devices.

Acknowledgments